ASTROBIOLOGY
Volume 9, Number 9, 2009

DOI: 10.1089/ast.2008.0329

Microbial Species Richness and Metabolic Activities in Hypersaline Microbial Mats: Insight into Biosignature Formation Through Lithification

Laura K. Baumgartner,[1,2] Christophe Dupraz,[1,3] Daniel H. Buckley,[4] John R. Spear,[5] Norman R. Pace,[2] and Pieter T. Visscher[1]

Abstract

Microbial mats in the hypersaline lake of Salt Pan, Eleuthera, Bahamas, display a gradient of lithification along a transect from the center to the shore of the lake. These mats exist under similar geochemical conditions, with light quantity and quality as the sole major environmental difference. Therefore, we hypothesized that the microbial community may be driving the differences in lithification and, by extension, mineral biosignature formation. The lithifying and non-lithifying mat communities were compared (via 16S rRNA gene sequencing, 485 and 464 sequences, respectively) over both temporal and spatial scales. Seven bacterial groups dominated in all the microbial mat libraries: bacteriodetes, alphaproteobacteria, deltaproetobacteria, chloroflexi, spirochaetes, cyanobacteria, and planctomycetes. The mat communities were all significantly different over space, time, and lithification state. Species richness is significantly higher in the non-lithifying mats, potentially due to differences in mat structure and activity. This increased richness may impact lithification and, hence, biosignature production. Key Words: Microbial mats—Lithification—Cyanobacteria—Hypersaline—Species richness—Biosignatures. Astrobiology 9, 861–874.

Introduction

Microbially induced carbonate precipitation is one of the main processes that leads to the formation of stromatolites, laminated organosedimentary carbonate deposits that provide some of the earliest evidence for life on Earth (Awramik, 1992). In stromatolites and some other microbial mats, microbially mediated precipitation results in the formation of organominerals (Perry *et al.,* 2007; Dupraz *et al.,* 2009). To qualify as biosignatures, organominerals need to contain chemical and structural characteristics of their microbial origin, including remnants of microbial cells or extracellular polymeric substances (EPS), other signatures of processes associated to microbial activity, or both (*e.g.,* stable isotopic fractionation or lipid biomarkers) (Cady *et al.,* 2003; Perry *et al.,* 2007). Because very few microbialites in Earth's rock record fulfill the first requirement of containing fossilized bacterial communities, a clear understanding of how to interpret biosignatures of processes is needed. It is also necessary to understand the role of contemporary microbial processes in the production of carbonate precipitation, lithification, and biominerals to detect and interpret these biosignatures in the rock record.

For calcium carbonate biosignatures, progress has been made in understanding microbe-carbonate interactions; studies have shown that certain species of microbes can promote precipitation and dissolution of carbonates through their metabolic effects on carbonate alkalinity. For instance, the metabolic reactions of cyanobacteria and sulfate-reducing bacteria appear to promote calcium carbonate precipitation, and those of aerobic heterotrophic bacteria and many sulfide-oxidizing bacteria promote dissolution (Pentecost and Riding, 1986; Walter *et al.,* 1993; Freytet and Verrecchia, 1998; Visscher *et al.,* 1998, 2000; van Lith *et al.,* 2002; Visscher and Stolz, 2005). Therefore, net precipitation and lithification should be a function of the combined metabolic activities of the microbial mat community, and research is needed to characterize the community interaction and the relationship that links species diversity and metabolic activity to carbonate precipitation and biosignature formation.

[1]Department of Marine Sciences, University of Connecticut, Groton, Connecticut.
[2]Department of Molecular, Cellular, and Developmental Biology, University of Colorado, Boulder, Colorado.
[3]Institute of Geology, University of Neuchâtel, Neuchâtel, Switzerland.
[4]Department of Crop and Soil Sciences, Cornell University, Ithaca, New York.
[5]Division of Environmental Science and Engineering, Colorado School of Mines, Golden, Colorado.

In addition to influencing the carbonate alkalinity through their metabolism, the microbial community also controls the formation, characteristics, and degradation of EPS, which play an intricate role in the production of calcium carbonate (Dupraz and Visscher, 2005). Cyanobacteria and other mat organisms produce EPS for several purposes, including attachment and stabilization, localization of extracellular processes such as quorum sensing, and protection from desiccation and other environmental changes (de Winder *et al.,* 1999; Decho, 2000; Wotton, 2004). Freshly produced EPS can bind cations such as Ca^{2+}, which lowers their concentration in solution and inhibits calcium carbonate precipitation (Kawaguchi and Decho, 2002a, 2002b; Gautret and Trichet, 2005; Perry *et al.,* 2005; Braissant *et al.,* 2007, 2009). The cation-binding capacity of the EPS can be reduced or oversaturated through several processes (including microbial degradation of EPS), which results in a local increase in free Ca^{2+} and precipitation of carbonate minerals (Kempe and Kazmierczak, 1994; Dupraz and Visscher, 2005; Visscher and Stolz, 2005; Dupraz *et al.,* 2009). Different organisms produce different forms of EPS under different conditions, with further effects on precipitation and lithification. For instance, highly labile forms of EPS may be rapidly turned over, with highly localized spatial and temporal effects on carbonate precipitation (Decho *et al.,* 2005; Braissant *et al.,* 2009). Additionally, other properties of the EPS (*e.g.,* amount, water content, and acidic group composition) can impact mineral nucleation, growth, and morphology (*e.g.,* Braissant *et al.,* 2003; Ben Chekroun *et al.,* 2004; Bosak and Newman, 2005; Ercole *et al.,* 2007). Therefore, the community structure and dynamics of EPS producers and consumers will affect precipitation, lithification, and biosignature formation.

Thus, precipitation of carbonate minerals in microbial mats is a net result of two major processes, both of which are coupled to metabolic activity and have an impact on the saturation index of the carbonate mineral: (1) changes in alkalinity that impact the carbonate concentration and (2) alterations of cation (Ca^{2+}) concentration through the binding capacity of EPS (Dupraz and Visscher, 2005; Visscher and Stolz, 2005; Dupraz *et al.,* 2009). To understand the mechanisms that drive lithification, the metabolic diversity of the microbial community must, therefore, be examined. Community structure as well as biogeochemical changes that result from feedback between the metabolic activities of the microbes and their environment must also be investigated. One way to measure differences in a community's structure is through its diversity. Diversity varies as a function of species richness, the number of species in a community, species evenness (*i.e.,* the relative number of representatives of each individual species) and species composition, the phylogenetic composition of species present. Thus, a community can have high species richness but low evenness (many species, but one or two are numerically dominant), low richness with high evenness (few species with similar numbers of individuals of each species), or any other combination. In microbial communities, individual species can have very different metabolic rates and effects, and richness can indicate the potential for a wider range of metabolic capabilities.

Here, we combine molecular and biogeochemical analyses of microbial communities in an investigation of lithifying and non-lithifying mats in Salt Pan, Eleuthera, Bahamas. The permanently submerged microbial mats in this hypersaline lake thrive under similar environmental conditions, yet they exhibit very different degrees of lithification (from a solid crust near shore to unconsolidated soft sediment in the middle of the lake) (Dupraz *et al.,* 2004). This led us to believe that differences in microbial community and activity create the differences in lithification. These mats have previously been examined with deltaproteobacterial-specific primers in a preliminary attempt to determine the diversity of sulfate-reducing bacteria in the lithifying and non-lithifying mats (Baumgartner *et al.,* 2006). To understand the communities more thoroughly, we created larger libraries from universal primers to determine the total diversity within the two mat types and examined multiple samples to examine spatial and temporal changes in microbial diversity within these mats. In addition, we performed extensive studies of metabolic microbial processes and determined physicochemical characteristics of the water column and the underlying microbial mats. Examination of the microbial diversity through space and time, along with biogeochemical analysis, allowed us to gain insight into the effects of diversity on the mechanisms of calcium carbonate precipitation and biosignature formation.

Materials and Methods

Site description

Salt Pan is a hypersaline lake on Eleuthera, Bahamas (25°24′N, 76°33′W) (Fig. 1), which has been characterized previously (Dupraz *et al.,* 2004). The lake level and salinity are mainly controlled by the equilibrium between rainfall and evaporation, though salinity and $\partial^{18}O$ values of precipitated carbonates suggest that there is some potential for freshwater or seawater intrusion (data not shown). The water is hypersaline [70–150 practical salinity units (PSU)] and turbid. Benthic microbial mats cover the sediment throughout Salt Pan, and mat characteristics have been examined along a transect from the center to the edges of the lake (Dupraz *et al.,* 2004). At the center of the lake, the 1–2 cm thick mats are gelatinous (EPS rich) with no precipitate (water depth 30–60 cm, depending on season, Fig. 1, Table 1). Shoreward, the mats undergo a sudden transition to a continuous lithified carbonate crust, which is 1–2 mm thick and always submerged (water depths of 10–30 cm during dry season, Fig. 1, Table 1). At the edge of the constantly submerged portion in the lake, the mats form a patchy carbonate crust, which was not sampled in this study.

Preliminary measurements have shown that both oxygen production and sulfate reduction are higher in the lithified mats than in the unlithified mats (Dupraz *et al.,* 2004). Additionally, although macroscopic observations of precipitation and pigment reveal obvious differences between the mat types, previous microscopic observations of morphologically conspicuous cyanobacteria indicated that *Gloeocapsa* sp. dominates the surface layers of all mat types and *Microcoleus* sp. dominates in the deeper layers (Dupraz *et al.,* 2004). However, these observations included only the most morphologically distinct biota, and the differences between the lithified and unlithified mats in microbial activity, pigment patterns, and particularly the presence or absence of lithification suggest fundamental differences in microbial community composition.

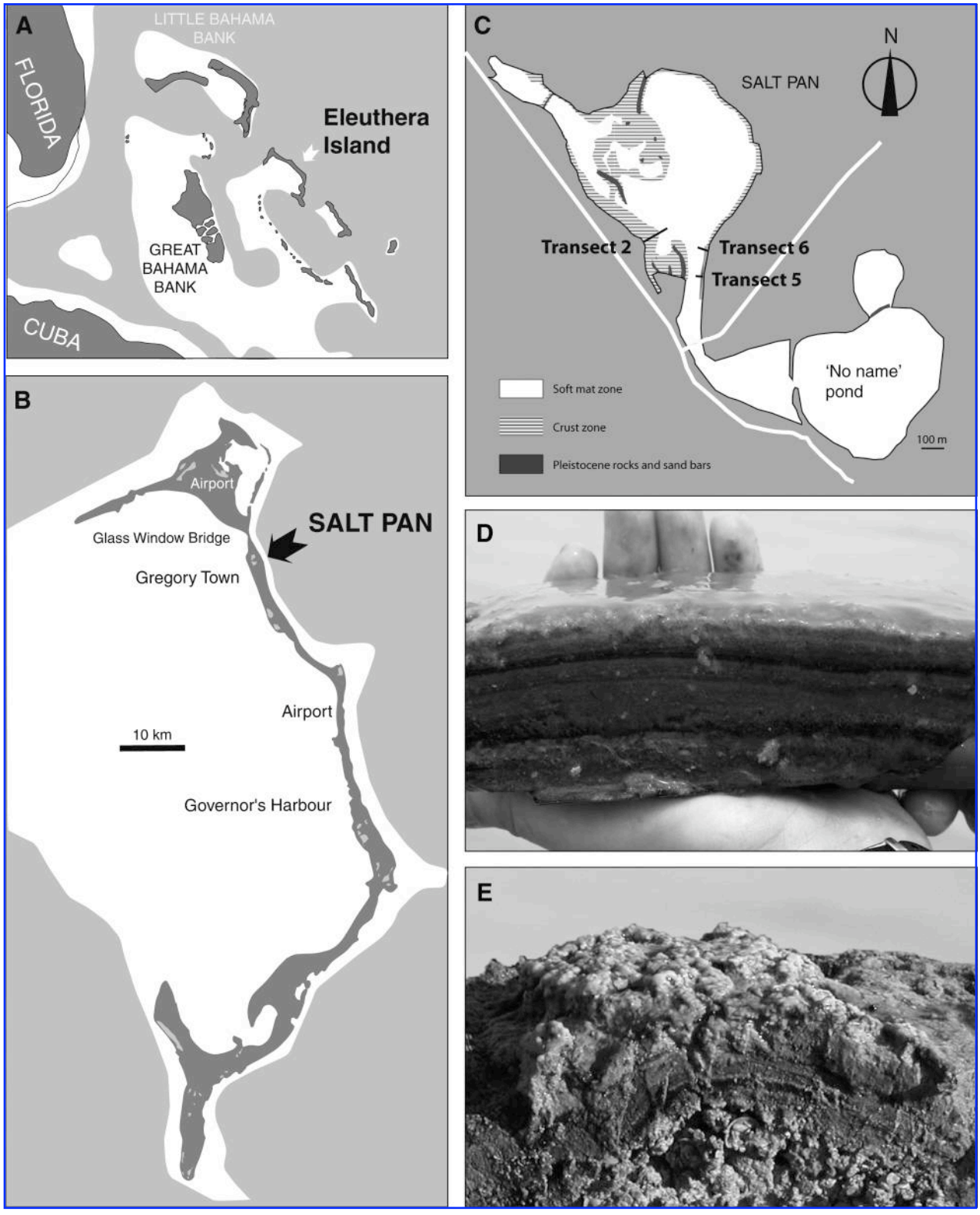

FIG. 1. Salt Pan, Eleuthera, Bahamas, with relevant transects and mat types. (**A**, **B**) General location of Eleuthera and Salt Pan. (**C**) Map of Salt Pan, with areas of lithifying and non-lithifying mat outlined. Transects discussed in this paper (2, 5, and 6) are indicated. Data is designated by transect, mat type (N = non-lithifying; L = lithifying, b = whole transect), and year (*e.g.*, 2N04 is the 2004 library from the transect 2 non-lithifying mat samples). (**D**) Non-lithifying mat, note the prevalence of surface EPS. (**E**) Lithifying mat, note the solid surface crust.

Table 1. Physicochemical Characteristics of Salt Pan, Eleuthera

	Winter (February–March)		Summer (June–September)	
	Soft mat	*Crusty mat*	*Soft mat*	*Crusty mat*
pH	8.3 ± 0.2 ($n = 24$)	8.3 ± 0.1 ($n = 24$)	8.3 ± 0.1 ($n = 19$)	8.4 ± 0.1 ($n = 19$)
T (°C)	27.8 ± 4.1 ($n = 28$)	28.9 ± 4.8 ($n = 28$)	29.5 ± 2.9 ($n = 22$)	31.1 ± 3.4 ($n = 22$)
Salinity (PSU)	85.9 ± 7.2 ($n = 18$)	90.3 ± 6.2 ($n = 18$)	87.5 ± 25.2* ($n = 15$)	95.9 ± 37.1* ($n = 15$)
Light (% surface irradiance)	2.8 ± 0.8 ($n = 8$)	10.9 ± 3.2 ($n = 8$)	3.7 ± 0.6 ($n = 6$)	12.2 ± 1.7 ($n = 6$)
Water depth at transition crusty-soft (cm)	36.4 ± 3.2 ($n = 14$)		29.6 ± 6.5* ($n = 11$)	

Observations were made between 8:30 a.m. and 1 p.m. during eleven field campaigns in the period from 2000 to 2008. Winter measurements were taken in February or March; summer readings represent the period June–September. Average ± standard deviation and number of observations (n) are given.

*Includes two June observations, which represent highest salinity (*ca.* 140–160 PSU) and temperature (*ca.* 34–36°C) and lowest water levels.

Environmental analyses

Measurements of pH, temperature, salinity, and light were taken along seven 30–60 m transects into the lake. Temperature and pH were measured with a Hanna HI 9024 portable meter. Salinity was measured via a handheld refractometer with a salinity scale (Fisher Scientific). Light (photosynthetically active radiation) was measured with a LI-COR LI-250 meter equipped with an underwater quantum sensor (LI-192 sensor), UVA and UVB were measured with a Solar Light PMA 2200 radiometer and an underwater UVA+B probe (PMA 2107-WP). Transects were sampled on June 2001; March 2003; February and July 2004; February, June, and September 2005; February and September 2006; and February and July 2007.

Sections of mat ($\sim 12 \times 12 \times 2.5$ cm) were removed from the lake and incubated in lake water for environmental analyses under ambient light and temperature conditions. During these analyses, light (photosynthetically active radiation) at the mat surface was measured with a LI-COR LI-250. Ambient light was regulated with a neutral-density screen to mimic *in situ* values at depth from measurements taken at Salt Pan during the initial sampling. Depth profiles of oxygen, sulfide, calcium, and pH were measured with rapid responding microelectrodes (Diamond General and Unisense), with use of a battery-driven micromanipulator and servo controlling system (National Aperture, Inc.). Activity of sulfate-reducing bacteria was analyzed with the "silver foil" technique (Visscher *et al.,* 2000), by which a vertically sliced mat sample was pressed against a sheet of silver foil that had been coated with ^{35}S-labeled sulfate. The sheet was incubated against the sample for 2–4 hours, allowing sulfate reduction to transform the labeled sulfate to sulfide, which binds to the silver. Unused $^{35}SO_4^{2-}$ was removed by rinsing the Ag foil, after which the distribution of radiolabeled sulfide ($Ag^{35}S$) was visualized by radiography (BioRad Molecular Imager System GS-525). The sulfide production measured in the foil experiments was calibrated to sulfate reduction rates with use of the conventional ^{35}S-sulfate incubations in individual mat layers (Jørgensen *et al.,* 1991; Visscher *et al.,* 1992).

Sampling and DNA sequencing

Mats were sampled on March 14, 2003, (Transect 2, Fig. 1) and July 27 and 28, 2004 (Transects 2 and 6). The nonlithifying mats were sampled by coring in triplicate with a 1.2 cm diameter stainless steel corer (triplicate samples cored from $\sim 1\,m^2$ area of mat). The harder lithifying mats were sampled in a large crust (10×10 cm), which was subsampled in triplicate for extraction. Samples were immediately chilled and frozen within 3 hours of sampling. They were then transported to the laboratory frozen and stored at −80°C. Mat sections were homogenized with a sterile pipette tip; then 0.1–0.3 g sections ($\sim 0.25\,cm^3$) underwent DNA extraction with the QBiogene FastDNA Spin Kit for Soil according to manufacturer's instructions, though 1.5 minutes of bead-beating were substituted for the 0.5 minutes of FastSpin.

Four water samples were taken from the middle of Transect 2 in Salt Pan on July 28, 2004. For each sample, 0.5 L of water was centrifuged in 50 ml increments (20 min at 6000 rpm) to create a cell pellet, which was then frozen and transported to the laboratory frozen and stored at −80°C. The pellet was homogenized with a pipette tip, and ~0.15 g was used for each triplicate DNA extraction as outlined above.

The 16S rRNA genes from these samples were amplified via polymerase chain reaction (PCR) with universal primers (515F and 1391R; Lane, 1991). PCR was conducted according to previously published methods (Spear *et al.,* 2005). PCR products from the triplicate samples were then pooled, cloned, screened by restriction fragment length polymorphism (RFLP), and sequenced as previously described (Spear *et al.,* 2005). The clone libraries generally contained >30 different patterns by RFLP, and all clones were sequenced.

Sequence analysis

Raw sequences were analyzed and assembled into contiguous sequences then compared to the GenBank database by the basic local alignment search tool (BLAST; Altschul *et al.,* 1990) with the XplorSeq software package (Frank, 2008). Contiguous sequences with BLAST bit scores of over 500 and lengths >300 bp were aligned with the NAST aligner to a database of >75,000 near full-length (>1250 nucleotide) sequences (DeSantis *et al.,* 2003, 2006). Aligned sequences were imported into the ARB software package (Ludwig *et al.,* 2004). Potential chimeric sequences were identified by long branch length in ARB and checked by examining each end of the sequence with the BLASTn function on the NCBI website (http://www.ncbi.nlm.nih.gov/BLAST; Altschul *et al.,* 1990). If the two ends of the sequence generated BLAST hits from

different genera, it was classified as a chimera and excluded from further analysis.

Differences in diversity between sequences from each library were analyzed with UniFrac (Luzapone and Knight, 2005) and ∫-LibShuff (Singleton *et al.*, 2001; Schloss *et al.*, 2004). Expected diversity from each library was calculated with EstimateS (Colwell, 2005). Matrices for EstimateS were filtered with lanemaskPH to remove distance caused by hypervariable regions (provided with ARB database; Hugenholtz, 2002). For the EstimateS calculations, we used 11 operational taxonomic unit (OTU) definitions, from 90% to 100% sequence identity, and we report the results from the 97% identity OTU [approximately species level (Stackebrandt and Goebel, 1994)]. Chao1 was calculated via the classic formula in EstimateS (Chao, 1984). Unique sequences were submitted to GenBank, accession numbers DQ423799–DQ424817. Data were designated by transect (see Fig. 1), mat type (N = non-lithifying; L = lithifying; b = whole transect), and year (*e.g.*, 2N04 is the 2004 library from the transect 2 non-lithifying mat samples). Sequences in NCBI were designated by sample zone/type (3 for lithifying and 4 for non-lithifying) and sequencing plate number. Thus, sequence designations for sample 2L03 start with either NE30, NE31, or NE32; those for 2N03 start with NE40, NE41, or NE42; those for 2L04 start with NE34, NE35, or NE36; those for 2N04 start with NE44, NE 45, or NE46; those for 6L03 start with NE35, NE36, or NE37; and those for 6N04 start with NE45, NE46, or NE47.

Results

Mat description

Two types of microbial mats from Eleuthera, lithifying and non-lithifying, were each sampled in triplicate from two different transects on opposite sides of Salt Pan. Each lithifying mat sample consisted of a very thin (1–2 mm thick) microbial mat overlain by a yellow, hard, knobby surface (1–2 mm thick). The thin microbial mat contained three colored layers: a green surface layer and closely interwoven red and black deep layers (Fig. 1A). A gray layer of carbonate mud with a few small shell fragments underlay the microbial mat. The entire mat profile above the underlying carbonate mud base (including the surface crust) was sampled for molecular analysis. The non-lithifying mat samples were thicker ($\sim$1–2 cm), with a green gelatinous surface layer with EPS ($\sim$0.5–1 cm) (Fig. 1B). The deeper layer of this mat was black (iron-sulfide rich), followed by the gray carbonate sediment. Again, the entire mat profile above the muddy sediment was sampled for molecular analysis. The mats were not subsampled by depth due to difficulties presented by their physical structure.

Environmental analyses

Temperature, salinity, pH, and light intensity were measured along seven transects through the lake between 2001 and 2008 (Table 1). Physicochemical observations for Transect 5, measured February 2005, are representative for the entire lake (Fig. 2) and similar to measurements taken when the 2003 molecular sampling was conducted. Several parameters were similar across the lithifying and non-lithifying mats: temperature at the mat surface was 33.9 to 35.8°C, pH remained steady at approximately 8.3 throughout the water column, and salinity ranged from 88 to 90 PSU. Light intensity changed with changing cloud conditions. Under cloudless conditions, which often prevail, the maximum light intensity at the water surface reached values of up to 2200 μE m^{-2} s^{-1}. We normalized light intensity at the mat surface by dividing that number by the light intensity at the water surface, which should remove effects of transient changes from clouds. Light intensity at the mat surface decreased as water depth increased, from 112 μE m^{-2} s^{-1} at 20 m from the shoreline (*ca.* 25 cm water depth; lithifying mat) down to 38 μE m^{-2} s^{-1} at 30 m into the lake (*ca.* 45 cm water depth; non-lithifying mats). Over 7 years, physicochemical data demonstrated a seasonal trend (Table 1).

Representative profiles of oxygen, sulfide, calcium, and pH in the lithifying and non-lithifying mats from February 16–17, 2005, are shown in Fig. 3. These profiles reflect the depth profiles observed during all the sampling dates. The daytime oxygen concentration in the lithifying mat is twice as high as the concentration in the non-lithifying mats. The oxygen concentration in both mats decreases at night, while sulfide concentration increases. Sulfide concentrations are higher in the lithifying mats than in the non-lithifying mats, and sulfide is found closer to the surface in these mats. Calcium concentrations are depressed at the surface of the lithifying mat, which corresponds with lithification in the mat profile. Note that differences between the depth profiles are not due to differences at the sediment-water boundary for the two different mats: the surface concentrations for the measured geochemical characteristics are similar for both mat types.

Representative sulfate reduction rates and oxygen production and consumption rates for the lithifying and non-lithifying mats are shown in Fig. 4 (measured February 16–19, 2006, similar to those measured on other dates). In the lithifying mats, oxygen production is two to seven times higher, and oxygen consumption is about three times higher than that observed in the non-lithifying mats. Sulfate reduction is also higher in the lithifying mat, particularly just above the lithified zone. Average sulfate reduction rates in the lithifying mats are 37.2 μM sulfate $hour^{-1}$, which is significantly different from the 7.7 μM sulfate $hour^{-1}$ in the non-lithifying mats ($n = 3$ for each mat type, $p < 0.05$ by Mann-Whitney test).

Molecular analysis

A total of 1019 16 rDNA gene sequences were analyzed from the mat libraries, including 948 from the universal primer pair and 116 from the delta96F primer pair. Seventy sequences were analyzed from the water library. Mat sequences had an average identity of 93% relative to sequences in GenBank (Fig. 5). The large number of sequences with low identity (Fig. 5) indicates that much of the diversity in these libraries consists of previously unsampled sequences and, therefore, unsampled organisms. The most common phylogenetic groups observed in each sample included bacteriodetes, alphaproteobacteria, deltaproteobacteria, chloroflexi, spirochaetes, cyanobacteria, and planctomycetes (Table 2). For the universal primer libraries, sampling coverage was analyzed with EstimateS, and collection curves for each of the libraries did not reach an asymptote (Table 2, collection curves not shown).

Sequences previously obtained with a deltaproteobacterial-specific primer pair (Baumgartner *et al.*, 2006) were not significantly different from those in the same clade obtained with

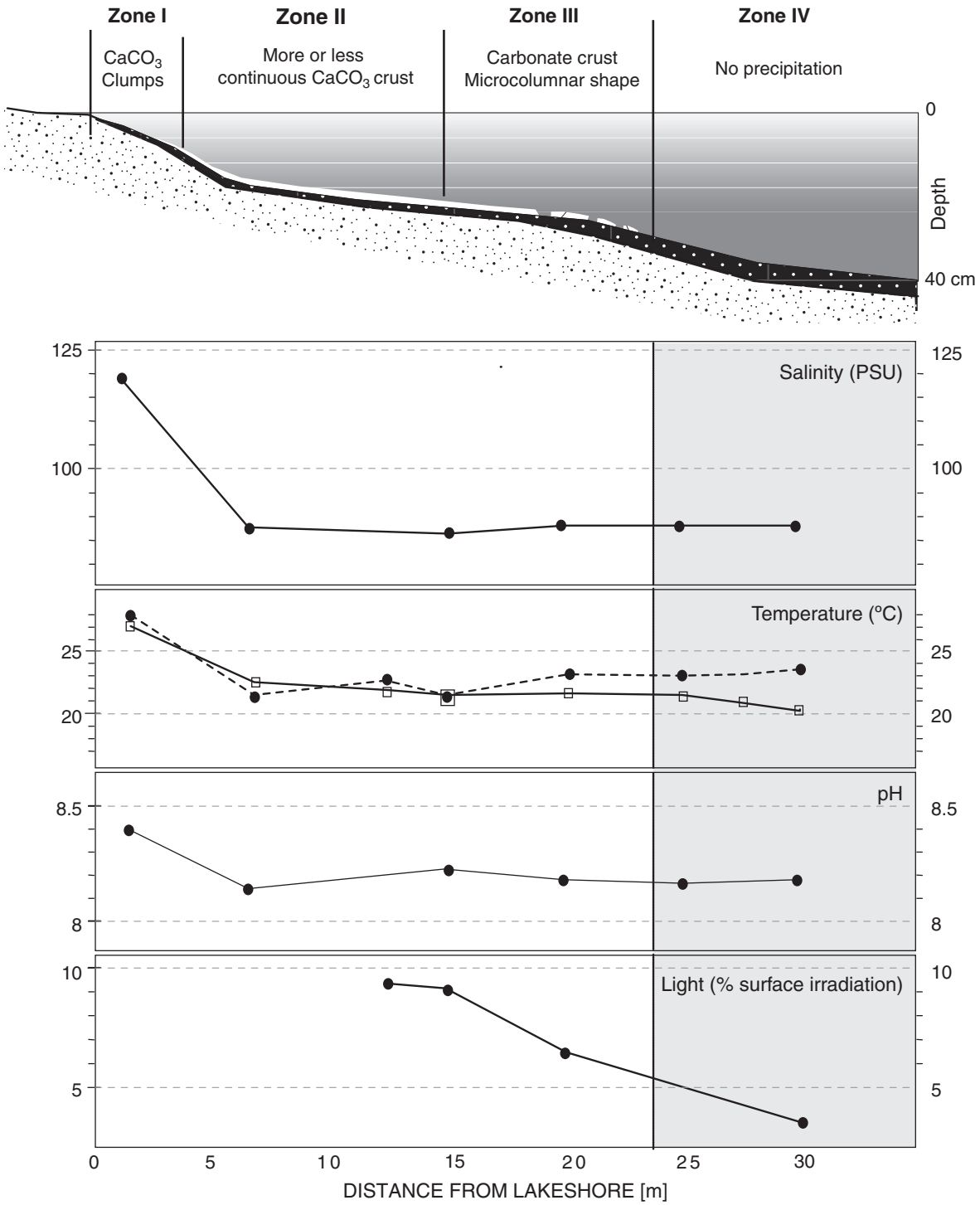

FIG. 2. Representative salinity, temperature, pH, and normalized light along transect, taken February 2005 on Transect 5 (5b05, but representative of what was seen at all sampling times). Top panel shows transect with mat types and approximate water depth. Surface water temperature is shown in open symbols and solid line; sediment surface water temperature is shown in closed symbols and dashed line. The vertical line represents the approximate transition from lithifying to non-lithifying mat. We normalized light intensity at the mat surface by dividing that number by the light intensity at the water surface, which should remove effects of transient changes due to cloud cover.

a universal primer pair (515F, 1391R) as revealed by Unifrac analysis (data not shown). This demonstrates that, for the groups targeted by both primers, primer bias was minimal. The delta96F sequences were not included in further analyses to avoid bias in the data set.

We hypothesized that diversity and community composition within the lithifying and non-lithifying microbial mats were affected by differences in time, transect location, and mat type. To examine these hypotheses, the libraries were analyzed with two statistical packages, UniFrac and

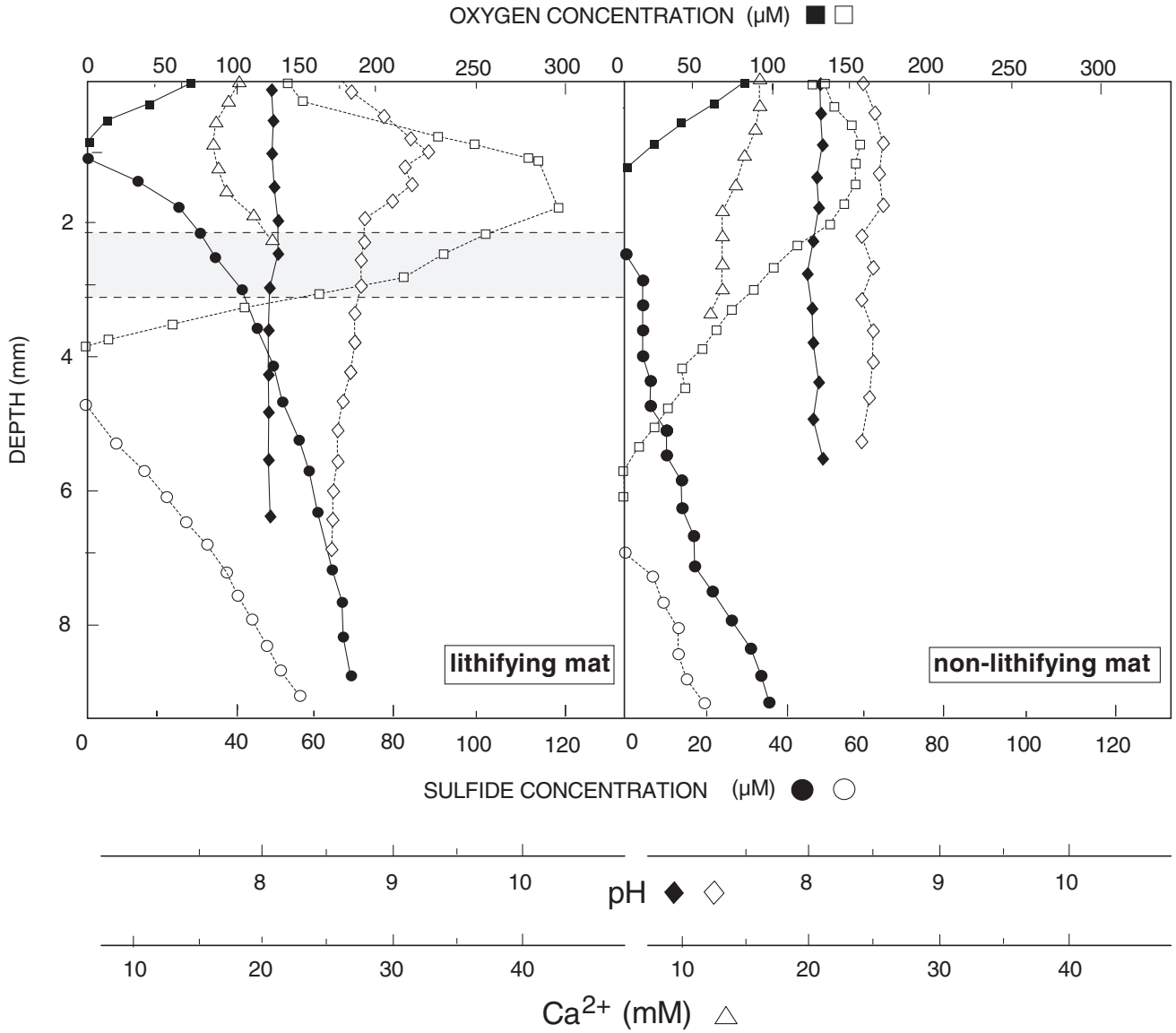

FIG. 3. Representative profile of O_2, S^{2-}, Ca^{2+}, and pH (data from Transect 5, February 2005, 5b05; but representative of observations from all sampling dates). Closed symbols represent nighttime profiles (*ca.* 4:00–5:00 a.m.). Open symbols are daytime profiles (12:30–2:30 p.m. Light intensity = 1850–2100 μE m^{-2} s^{-1}). Horizontal lines represent the approximate location of the lithified crust.

∫-LibShuff. The sequence composition of each library was distinct, as revealed in pairwise tests, and these differences in composition were significant [UniFrac ($p = 0.00$) and ∫-LibShuff ($p < 0.01$)]. The interrelationship of the libraries was examined with the UPGMA cluster function in Unifrac (Luzapone and Knight, 2005), and UPGMA trees were constructed from 115 randomly subsampled sequences from each mat library or 70 randomly subsampled sequences from the mat and water libraries. Although the community observed in the microbial mats differed considerably from that observed in the water samples, the mat libraries did not cluster by time, location, or mat type (data not shown).

Lithifying versus non-lithifying mat communities

We sampled three pairs of lithifying and non-lithifying mats to determine the effect of mat type on microbial community composition. Each member of these mat pairs was significantly different from its counterpart by all methods applied in ∫-LibShuff and UniFrac. Likewise, ∫-LibShuff also revealed that differences in community composition between lithified and non-lithified mats were significant when sequences from different samples were pooled with respect to mat type ($p = 0.001$). A comparison of the most prevalent groups observed in all lithifying mats relative to those observed in non-lithifying mats is shown in Fig. 6. There are significant differences in group abundance between each pair of mats and when sequences are pooled with respect to mat type (Figs. 6, 7, 8).

Richness also varied considerably with respect to mat type, and non-lithifying mats generally had greater richness than lithifying mats (Table 2). This trend is significant for the comparison of 2L04 and 2N04 (Table 2), but not for comparison of 2L03 and 2N03, 6L03, or 6N03 (Table 2). This

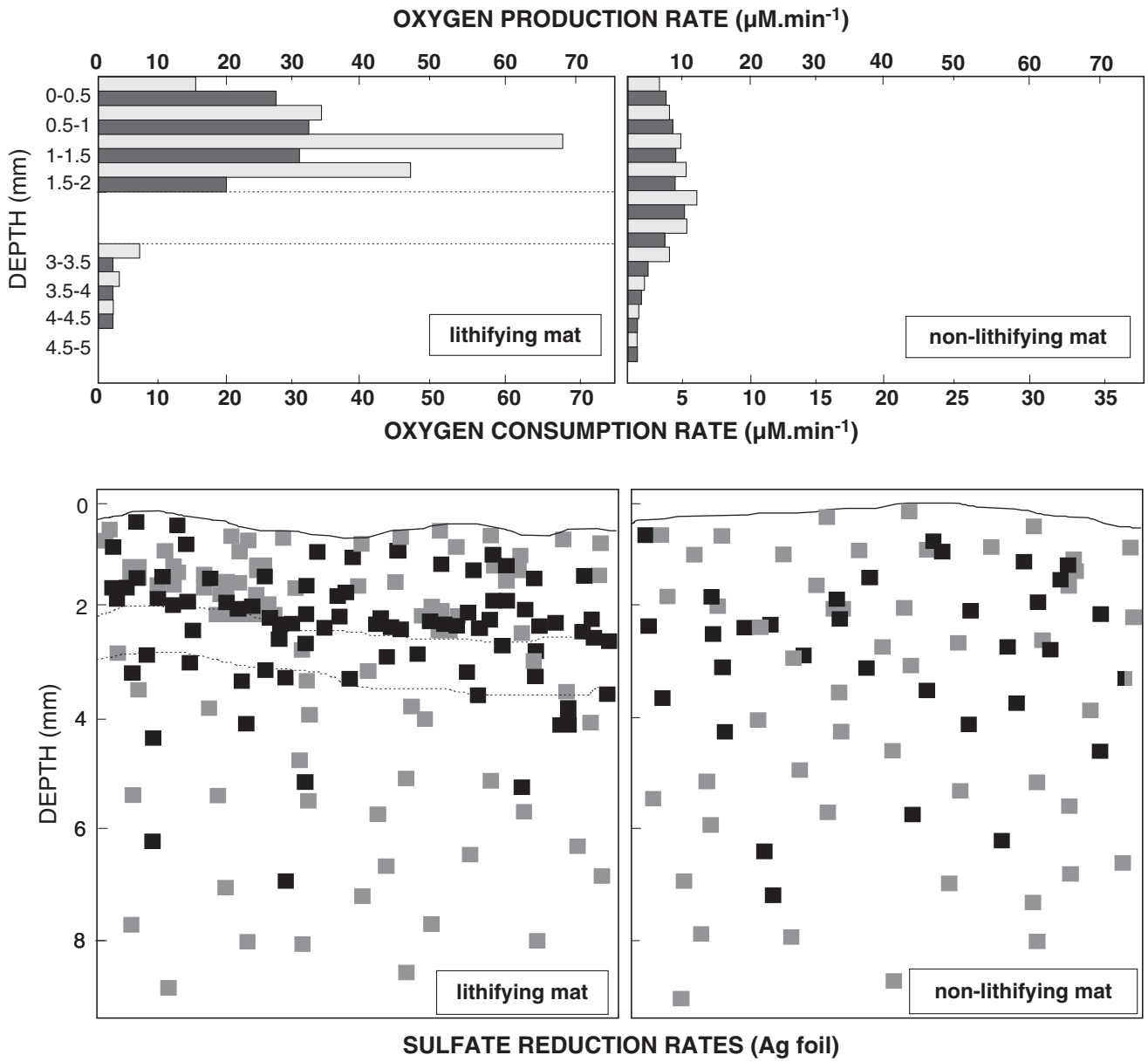

FIG. 4. Top panel: Oxygen production and consumption rates. Gray bars represent net O_2 production. Black bars represent total O_2 consumption (the sum of aerobic respiration, microbial sulfide oxidation, and chemical consumption). Bottom panel: Sulfate reduction rates in a profile of the mats. Pixels indicate areas of sulfate reduction (*i.e.,* $Ag^{35}S$ present); darker pixels indicate more reduction than gray pixels. Dotted lines indicate the upper and lower boundaries of the lithified layer in this sample.

result suggests that the effect of mat type on richness interacts either with the effects of time or transect location. When the libraries are pooled by mat type with respect to transect location (2 vs. 6) or time (2003 vs. 2004), and sample size differences are removed by random subsampling, differences in richness between the different mat types are significant (Table 2).

Temporal variation in communities (2b03 vs. 2b04)

We analyzed libraries obtained from Transect 2 in 2003 and 2004 to examine the degree to which mat community composition changes over time in the lake. For this analysis, sequences from different mat types were pooled to represent each different time. A comparison of these libraries revealed a few differences in community structure (Fig. 7). Generally, there are more alphaproteobacterial sequences in 2004 libraries and more planctomycete and spirochaete sequences in 2003 libraries. The Transect 2 samples are all significantly different by all the pairwise methods used. In addition, there is a large, though not significant, difference in species richness between the 2003 and 2004 libraries for randomly subsampled libraries of 268 sequences for 2003 and 2003 (Table 2). Time appears to affect species richness, but further sampling would be required to confirm this effect.

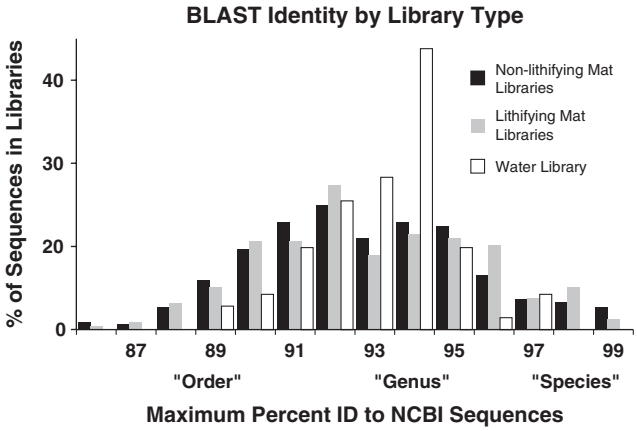

FIG. 5. Sequence identity for all the sequences sampled in this study relative to sequences currently present in GenBank.

Spatial variation in communities (2b04 vs. 6b04)

In 2004, we examined mat samples from opposite sides of the lake (Transects 2 and 6) to determine the effect of location on diversity. For this analysis, sequences from different mat types were pooled by transect (Fig. 8). There are more alphaproteobacteria and cyanobacteria in the Transect 2 libraries and more chloroflexi and bacteroidetes in the Transect 6 libraries, but these differences are controlled by a single library in each instance (Table 3). There is also very little difference in species richness between the libraries when pooled by transect (Fig. 8). Therefore, there are no obvious differences in species richness or abundance by location.

Discussion

We conducted biogeochemical and molecular community analysis on lithifying and non-lithifying mats from a hypersaline lake (Salt Pan, Eleuthera) to determine whether differences in geochemical and physical parameters, community activity, or community structure were major drivers of the formation of this biosignature. The majority of the environmental parameters were similar across both mat types, though the non-lithifying mats are deeper in the lake and thus exposed to less light (Fig. 2, Table 1).

Profound biogeochemical differences were observed between lithifying and non-lithifying mats. Non-lithifying mats were observed to have lower metabolic rates than lithifying mats with respect to oxygen production/consumption and sulfate reduction (Figs. 3, 4). These differences were accompanied by differences in microbial community structure both in terms of community composition and richness. Although community composition in lithifying mats differed significantly from that in non-lithifying mats, high spatial and temporal variability was observed in the mat system that made it impossible to associate particular community assemblages or the abundance of particular microbial groups with the process of lithification.

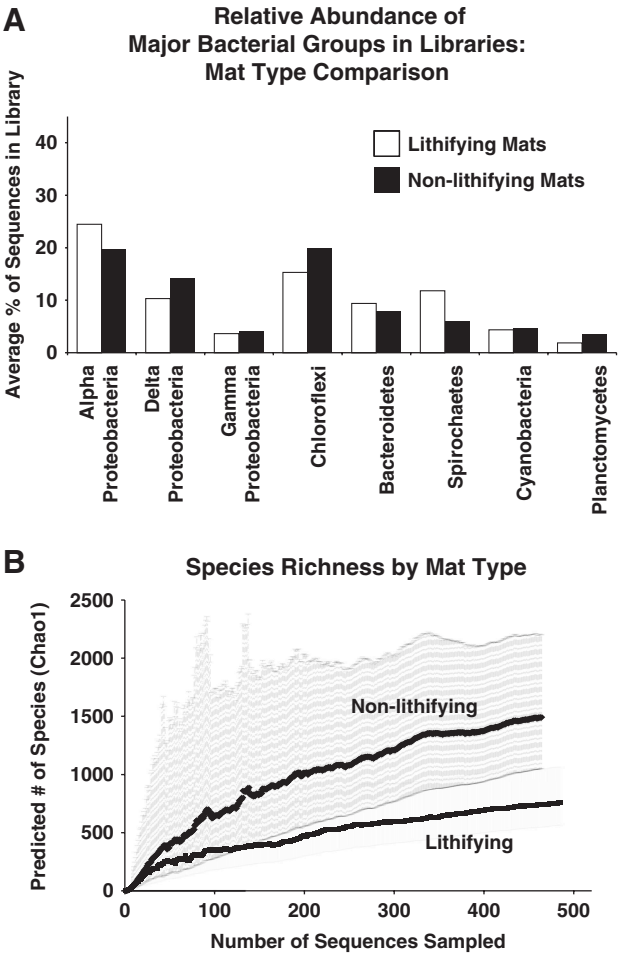

FIG. 6. Variation in mat community structure by mat type (lithifying vs. non-lithifying). (**A**) Relative abundances of dominant bacterial groups. (**B**) Chao1 collection curves from EstimateS (97% OTU). Error bars indicate 95% confidence intervals.

Table 2. Diversity Estimates for Mat Samples Calculated from 16S rRNA Gene Libraries

Sample	*Sequences analyzed*	*OTU*	*ACE*	*Chao1*	*Chao1 95% C.I.*
2L03	186	112	740	535	317/984
2N03	222	157	776	605	409/951
2L04	141	65	135	121	90/190
2N04	127	72	735	734	285/2130
6L04	158	87	352	361	221/668
6N04	115	106	379	380	220/727
Water	70	9		17	10/74
Pooled libraries:					
All non-lithifying	464	292	1949	1492	1048/2198
All lithifying	485	240	844	756	564/1062
2L03 and 2L04	327	168	619	484	351/714
2N03 and 2N04	327	212	1300	1256	799/2069
2L04 and 2L06	223	121	332	311	223/474
2N04 and 2N06	223	145	1222	926	536/1708
2b03	268	184	1007	954	612/1571
2b04	268	131	530	403	280/629
6b04	268	166	689	568	399/861

EstimateS, OTU defined at a 0.03 dissimilarity cutoff.

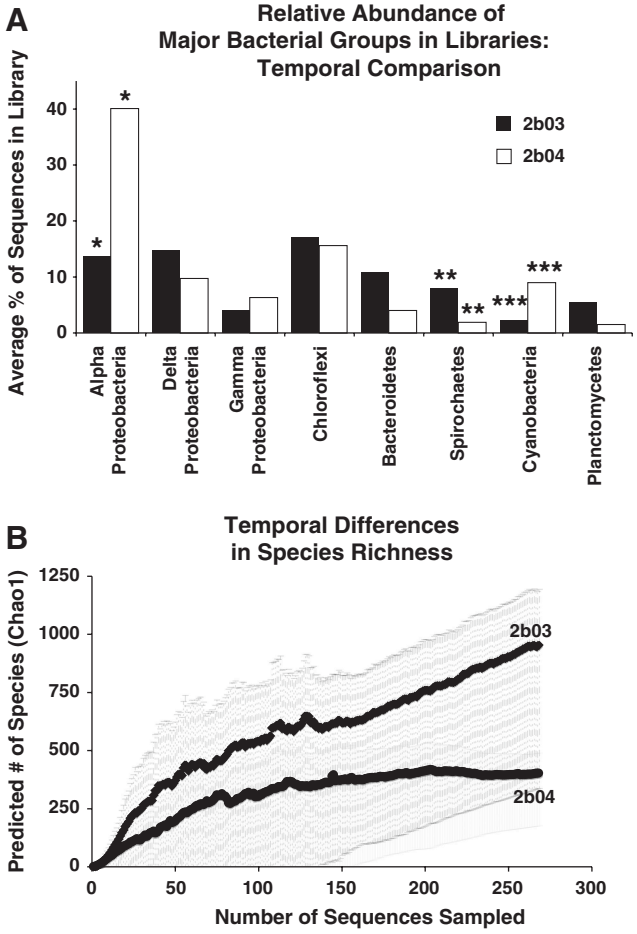

FIG. 7. Temporal variation in mat community structure. (**A**) Relative abundances of dominant bacterial groups. Asterisks denote differences between libraries found to be significant with use of Fisher's exact test with Bonferroni correction for multiple comparisons of all lithifying and non-lithifying mat sample pairs ($P < 0.0001$). (**B**) Chao1 collection curves from EstimateS (97% OTU). Error bars indicate 95% confidence intervals.

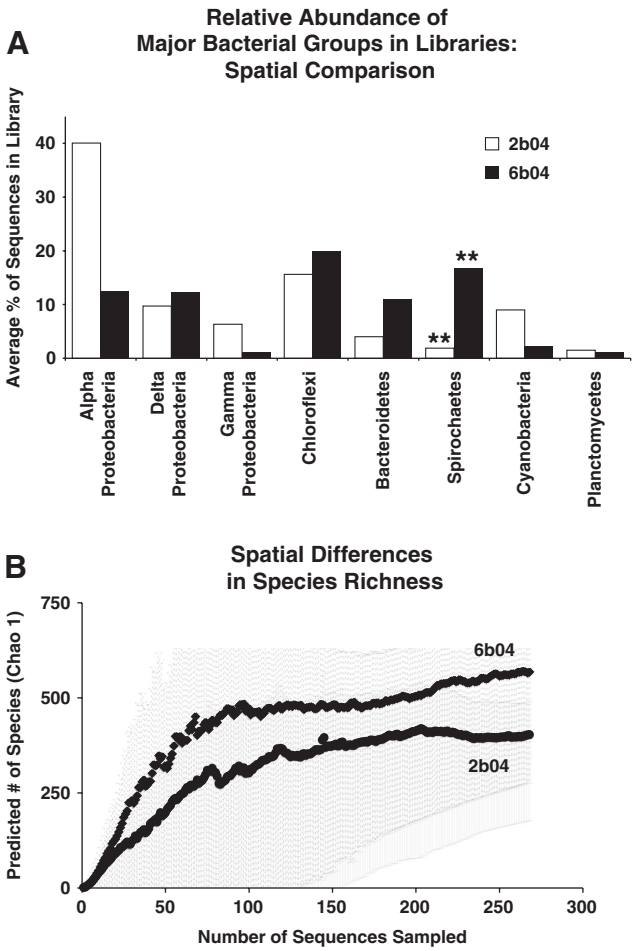

FIG. 8. Spatial variation in mat community structure. (**A**) Relative abundances of dominant bacterial groups. Asterisks denote differences between libraries found to be significant with use of Fisher's exact test with Bonferroni correction for multiple comparisons of all lithifying and non-lithifying mat sample pairs ($P < 0.0001$). (**B**) Chao1 collection curves from EstimateS (97% OTU). Error bars indicate 95% confidence intervals.

Potential effects of depth and light on element cycling

Depth and light are the primary environmental variables that correspond with differences in mat lithification in Salt Pan [Figs. 2, 3 (surface measurement)]. In the relatively well-mixed lake, the main effect of depth is its influence on the amount of light that reaches the mat surface. There are several mechanisms by which light intensity may influence lithification potential. If the higher irradiance on the shallower lithifying mats in Salt Pan results in faster photolysis of EPS by light, then EPS would be more accessible for microbial degradation. Although EPS is generally only a small percentage of the organic carbon output by cyanobacteria, and much of photosynthate is readily consumable low–molecular weight organic carbon (Decho *et al.,* 2005; Braissant *et al.,* 2009), the photolysis of EPS in the shallower, lithifying mats would add shorter (more labile) polysaccharide fragments to the system. This could increase the rate of oxygen consumption, which would increase both direct consumption by aerobic heterotrophs and indirect consumption via oxidation of the sulfide produced by sulfate reduction, two processes that play almost equally important roles in labile EPS degradation (Braissant *et al.,* 2009). Furthermore, if photosynthesis is not light-saturated, additional irradiance would increase the rate of photosynthesis (which is higher in the lithifying mats) and, thus, increase the production of EPS, low–molecular weight carbon, and oxygen.

Effects of rapid cycling on lithification and species richness

If light drives more rapid elemental cycling within the lithifying Salt Pan mats, the result could be more rapid production and consumption of EPS. As was discussed in the Introduction, higher EPS production and consumption rates alter binding and release of calcium, create nucleation sites for calcium carbonate, and increase the local effects each metabolism has on local carbonate activity. This would create rapidly fluctuating changes in calcium and carbonate activity in the lithifying mats and, thus, rapid local fluctua-

Table 3. Abundance of Major Phyla Recovered in Clone Libraries from Each Stromatolite Type and Water Samples

	Percentage of sequences in library							*% of all libraries*
	2L03	*2N03*	*2L04*	*2N04*	*6L04*	*6N04*	*Water*	
Bacteria	94.1	96.3	99.3	96.1	89.7	87.0	100.0	94.4
Proteobacteria	33.9	31.0	54.7	58.3	27.7	26.1	87.1	41.1
Alphaproteobacteria	14.0	13.4	43.9	36.2	15.5	9.6	84.3	25.4
Deltaproteobacteria	18.3	11.1	2.9[a]	16.5[a]	9.7	14.8	2.9	11.6
Gammaproteobacteria	1.6	6.5	7.9	4.7	1.3	0.9		3.7
Chloroflexi	31.7[b]	2.3[b]	11.5	19.7	2.6[c]	37.4[c]		15.1
Bacteroidetes	2.2[d]	19.4[d]	7.2	0.8	18.7[e]	3.5[e]	1.4	9.0
Spirochaetes	4.8	11.1	2.2	1.6	28.4[e]	5.2[e]		8.7
Cyanobacteria	1.1	3.2	10.1	7.9	1.9	2.6		3.9
Planctomycetes	2.2	8.8	2.2	0.8	1.3	0.9		3.0
Verrucomicrobia		3.2	4.3		0.6		10.0	2.1
WS3	1.6	1.9		1.6	2.6	1.7		1.5
Firmicutes	0.5	2.3	2.9	0.8		2.6	1.4	1.5
OD2		5.1						1.1
Gemmatimonadetes	1.1	2.3	0.7			0.9		1.1
Haloanaerobales	1.6			0.8	2.6	0.9		0.9
Actinobacteria	1.6	0.5	0.7	2.4		0.9		0.9
Deferribacteres	2.7					2.6		0.8
Chlamydiae	0.5	2.3	0.7					0.7
Acidobacteria	3.2			0.8				0.7
OD1	0.5	1.9						0.5
Nitrospirae	1.6					0.9		0.4
AC1	1.6							0.4
Lentispaerae		0.5						0.1
BRC1		0.5						0.1
OP8	0.5							0.1
Other bacteria	1.1		2.1	0.8	3.2	0.9		1.2
Archaea total	5.9	3.7	0.7	3.9	10.3	13.0		5.6
Eukarya total		2.8	1.4			2.6		1.1

Footnotes denote differences between libraries found to be significant with use of Fisher's exact test with Bonferroni correction for multiple comparisons of all lithifying and non-lithifying mat sample pairs ($P < 0.0001$).

[a]Deltaproteobacteria are more abundant in 2N04 than in 2L04.

[b]Chloroflexi are more abundant in 2L03 than 2N03.

[c]Chloroflexi are more abundant in 6N04 than in 6L04.

[d]Bacteroidetes are more abundant in 2N03 than 2L03.

[e]Bacteroidetes and Spirochaetes are more abundant in 6L04 than in 6N04.

tions in calcium carbonate saturation, which would potentially favor net precipitation. Additional degradation of EPS also would decrease the oxygen concentration. In the resulting anoxic environment, the remaining carbon would be utilized by sulfate-reducing bacteria, whose metabolism further favors carbonate precipitation (Visscher *et al.,* 2000; Braissant *et al.,* 2009).

This rapidly changing environment could limit the species richness, which would leave only certain niches open to those organisms that have the physiological ability to adapt to the changes. Although the large-scale community structure is similar between all Salt Pan mats (Table 2), the statistical methods found significant differences in phylogenetic composition between mat types, between communities from different transects, and between different times. The overall mat environment is selecting at what is, essentially, the phylum level, but the dominant members of each of the phyla that are present differ between the mats. Rapid elemental cycling in the lithifying mats may select for key types of organisms, which have high metabolic rates under rapidly changing environmental conditions (have phenotypic plasticity).

The non-lithifying mats undergo smaller daily geochemical changes and, therefore, less selection toward plasticity. Additionally, the non-lithifying mats are thicker, and the greater depth of the non-lithifying mats may create more microhabitats and more stable environments, which also allows for greater species richness. Most microbial mats that produce modern microbialites are generally rather thin, and the newly produced carbonate crust serves as a physical substrate. Although thick microbial mats (*i.e.,* many centimeters in thickness) may show small pockets of precipitation (Jørgensen and Cohen, 1977; Jørgensen *et al.,* 1983), most of them never form continuous crusts or emerging microbialite formations (*e.g.,* stromatolites, thrombolites). Most of the production and consumption of EPS in the Salt Pan non-lithifying mat is concentrated in the first top centimeter (Braissant *et al.,* 2009). Clearly, incomplete EPS turnover in the thick non-lithifying mat of Salt Pan (related to either greater production or less degradation) leads to greater accumulation of EPS, which contributes to cation binding and inhibition of precipitation. The result is an accumulation of large amounts of "non-metabolized" organic carbon with

depth that will never lithify. The greater species richness in the thick non-lithifying mats may increase EPS production but does not appear to increase degradation.

Temporal variation in the mat communities

Overall, the community compositions of the microbial mats are very complex, and they are undersampled in this study. However, when the libraries were analyzed at the current sampling level, all the libraries were significantly different from each other by most statistical methods. There are no apparent trends in the abundance of one group in the libraries or in overall community structure by time of sampling or mat location.

At the current sampling levels, the 2003 libraries appear to have higher species richness than the 2004 libraries (Table 2). Most likely these differences result from temporal changes in temperature and salinity. Given the differential effects of different types of metabolism on carbonate precipitation and dissolution, these changes could affect precipitation as well, and further measurements are needed to examine these changes.

Spatial variation in the mat communities—a light-driven continuum?

Similarly, the statistical data suggest that mats of the same type from across the lake have different communities. However, all the measured geochemical and physicochemical constituents have similar values between the transects when measured at similar mat types (*i.e.,* in and above lithifying and non-lithifying mats), though there could be differences in a compound that was not measured. Although neither side of the lake is shaded, the mats on either side may receive different amounts of light, particularly due to slight differences in water depth. If there are continuous light differences, this could result in difference in lithification. However, it is likely that the mat continuum is controlled by light, and the lithifying/non-lithifying transition exists at a point that receives a certain amount of irradiance—which may be a different point on each side of the lake.

This conceptual model could be taken further, and there could be differences in lithification along the depth continuum, with greatest lithification at some optimum depth. Species richness, bacterial activity, and community composition may also change along this continuum, and this could be sampled. We may not have sampled at the exact same point on this continuum for each of the molecular samples, which may explain the overlying complexity of the molecular analysis (and differences between samples at the same location at different time points).

Conclusions

The community structure of the mat libraries is complex, yet it is critical to evaluate the species diversity carefully. This species (and metabolic) diversity in combination with geochemical characteristics (including EPS properties) of the mats are the key to understanding production of mineral biosignatures. Although similar bacterial groups are represented in all the mat libraries, the individual representatives of each group are different, which results in significant statistical differences between the mat communities. More intensive sampling would be needed to understand fully the community structure of these mats, but the current data are indicative of the dominant groups in each mat sample. Previously, Dupraz *et al.* (2004) proposed a carbon cycle for these mats, including cyanobacteria, heterotrophs, sulfate-reducing bacteria, and colorless sulfide-oxidizing bacteria. All these groups are well represented in the libraries, with two exceptions: the cyanobacteria are not abundant in the libraries, and known relatives of the colorless sulfide-oxidizing bacteria were not observed, though purple and green nonsulfur bacteria (that can perform similar metabolic functions) were. The appearance of sequences related to these groups supports the previously presented model.

Overall, increased activity and decreased species richness in the lithifying mats compared to the non-lithifying mats may be driven by the greater quantity of light that the lithifying mats receive. Thus, our results indicate avenues for further sampling. Along-transect differences in diversity and geochemistry should be examined for an area of maximum productivity/lithification, which may provide further clues as to the environmental and community requirements for lithification. Continued monitoring of changes in the mat communities with time may also provide clues as to the environmental drivers of lithification and, hence, mineral biosignature formation. Finally, if molecular methods become adapted for smaller template quantities or better methods become available for subsampling the millimeter-scale layers of the lithifying mats, a comparison of the lithifying mat diversity with depth would provide more information about key groups for lithification.

Acknowledgments

This work was sponsored by NSF EAR 0311929 and NASA JRI through Ames Research Center awarded to P.T.V. and Swiss National Fund grant 108141 awarded to C.D. We thank the crew of the R/V Walton Smith for logistic support. This is publication 16 of UConn's Center for Integrative Geosciences.

Disclosure Statement

No competing financial interests exist for any of the authors.

Abbreviations

BLAST, basic local alignment search tool; EPS, extracellular polymeric substances; OTU, operational taxonomic unit; PCR, polymerase chain reaction; PSU, practical salinity units; RFLP, restriction fragment length polymorphism.

References

Altschul, S.F., Gish, W., Miller, W., Myers, E.W., and Lipman, D.J. (1990) Basic local alignment search tool. *J. Mol. Biol.* 215:403–410.

Awramik, S.M. (1992) The oldest records of photosynthesis. *Photosyn. Res.* 33:75–89.

Baumgartner, L.K., Reid, R.P., Dupraz, C., Decho, A.W., Buckley, D.H., Spear, J.R., Przekop, K.M., and Visscher, P.T. (2006) Sulfate reducing bacteria in microbial mats: changing paradigms, new discoveries. *Sediment. Geol.* 185:131–145.

Ben Chekroun, K., Rodriguez-Navarro, C., Gonzales-Munoz, M.T., Arias, J.M., Cultrone, G., and Rodriguez-Callego, M.

(2004) Precipitation and growth morphology of calcium carbonate induced by *Myxococcus xanthus:* implications for recognition of bacterial carbonates. *Journal of Sedimentary Research* 74:868–876.

Bosak, T. and Newman, D.K. (2005) Microbial kinetic controls of calcite morphology in supersaturated solutions. *Journal of Sedimentary Research* 75:190–199.

Braissant, O., Cailleau, G., Dupraz, C., and Verrecchia, E.P. (2003) Bacterially induced mineralization of calcium carbonate in terrestrial environments: the role of exopolysaccharides and amino acids. *Journal of Sedimentary Research* 73:485–490.

Braissant, O., Decho, A.W., Dupraz, C., Glunk, C., Przekop, K.M., and Visscher, P.T. (2007) Exopolymeric substances of sulfate-reducing bacteria: interactions with calcium at alkaline pH and implications for formation of carbonate minerals. *Geobiology* 5:401–411.

Braissant, O., Decho, A.W., Przekop, K.M., Gallagher, K.L., Glunk, C., Dupraz, C., and Visscher, P.T. (2009) Characteristics and turnover of exopolymeric substances in a hypersaline microbial mat. *FEMS Microbiol. Ecol.* 67:293–307.

Cady, S.L., Farmer, J.D., Grotzinger, J.P., Schopf, J.W., and Steele, A. (2003) Biosignatures and the search for life on Mars. *Astrobiology* 3:351–368.

Chao, A. (1984) Non-parametric estimation of the number of classes in a population. *Scandinavian Journal of Statistics* 11:265–270.

Colwell, R.K. (2005) *EstimateS: Statistical Estimation of Species Richness and Shared Species from Samples,* Version 7.5. Available online at http://purl.oclc.org/estimates.

de Winder, B., Staats, N., Stal, L.J., and Paterson, D.M. (1999) Carbohydrate secretion by phototrophic communities in tidal sediments. *J. Sea Res.* 42:131–146.

Decho, A.W. (2000) Microbial biofilms in intertidal systems: an overview. *Continental Shelf Research* 20:1257–1273.

Decho, A.W., Visscher, P.T., and Reid, R.P. (2005) Production and cycling of natural microbial exopolymers (EPS) within a marine stromatolite. *Palaeogeogr., Palaeoclimatol., Palaeoecol.* 219:71–86.

DeSantis, T.Z., Dubosarskiy, I., Murray, S.R., and Andersen, G.L. (2003) Comprehensive aligned sequence construction for automated design of effective probes (CASCADE-P) using 16S rDNA. *Bioinformatics* 19:1461–1468.

DeSantis, T.Z., Hugenholtz, P., Keller, K., Brodie, E.L., Larsen, N., Piceno, Y.M., Phan, R., and Andersen, G.L. (2006) NAST: a multiple sequence alignment server for comparative analysis of 16S rRNA genes. *Nucleic Acids Res.* 34:W394–399.

Dupraz, C. and Visscher, P.T. (2005) Microbial lithification in marine stromatolites and hypersaline mats. *Trends Microbiol.* 13:429–438.

Dupraz, C., Visscher, P.T., Baumgartner, L.K., and Reid, R.P. (2004) Microbe-mineral interactions: early carbonate precipitation in a hypersaline lake (Eleuthera Island, Bahamas). *Sedimentology* 51:745–765.

Dupraz, C., Reid, R.P., Braissant, O., Decho, A.W., Norman, R.S., and Visscher, P.T. (2009) Processes of carbonate precipitation in modern microbial mats. *Earth-Science Reviews* 96:141–162.

Ercole, C., Cacchio, P., Botta, A.L., Centi, V., and Lepidi, A. (2007) Bacterially induced mineralization of calcium carbonate: the role of exopolysaccharides and capsular polysaccharides. *Microsc. Microanal.* 13:42–50.

Frank, D.N. (2008) XplorSeq: a software environment for integrated management and phylogenetic analysis of metagenomic sequence data. *BMC Bioinformatics* 9:1–16.

Freytet, P. and Verrecchia, E.P. (1998) Freshwater organisms that build stromatolites: a synopsis of biocrystallization by prokaryotic and eukaryotic algae. *Sedimentology* 45:535–563.

Gautret, P. and Trichet, J. (2005) Automicrites in modern cyanobacterial stromatolitic deposits of Rangiroa, Tuamotu Archipelago, French Polynesia: biochemical parameters underlaying their formation. *Sediment. Geol.* 178:55–73.

Hugenholtz, P. (2002) Exploring prokaryotic diversity in the genomic era. *Genome Biol.* 3, reviews 0003.1–0003.8.

Jørgensen, B.B. and Cohen., Y. (1977). Solar Lake (Sinai). 5. The sulfur cycle of the benthic cyanobacterial mats. *Limnol. Oceanogr.* 22:657–666.

Jørgensen, B.B., Revsbech, N.P., and Cohen, Y. (1983) Photosynthesis and structure of benthic microbial mats: microelectrode and SEM studies of four cyanobacterial communities. *Limnol. Oceanogr.* 28:1075–1093.

Jørgensen, B.B., Fossing, H., Wirsen, C.O., and Jannasch, H.W. (1991) Sulfide oxidation in the anoxic Black Sea chemocline. *Deep-Sea Research* 38:S1083–S1103.

Kawaguchi, T. and Decho, A.W. (2002a) A laboratory investigation of cyanobacterial extracellular polymeric secretions (EPS) in influencing $CaCO_3$ polymorphism. *J. Cryst. Growth* 240:230–235.

Kawaguchi, T. and Decho, A.W. (2002b) Characterization of extracellular polymeric secretions (EPS) from modern soft marine stromatolites (Bahamas) and its inhibitory effect on $CaCO_3$ precipitation. *Prep. Biochem. Biotechnol.* 32:51–63.

Kempe, S. and Kazmierczak, J. (1994) The role of alkalinity in the evolution of ocean chemistry, organization of the living systems and biocalcification processes. *Bulletin de L'Institut Oceanographique Monaco* 13:61–117.

Lane, D.J. (1991) 16S/23S rRNA sequencing. In *Nucleic Acid Techniques in Bacterial Systematics,* edited by E. Stackebrandt and M. Goodfellow, Wiley, New York, pp 115–175.

Ludwig, W., Strunk, O., Westram, R., Richter, L., Meier, H., Yadhukumar, Buchner, A., Lai, T., Steppi, S., Jobb, G., Förster, W., Brettske, I., Gerber, S., Ginhart, A.W., Gross, O., Grumann, S., Hermann, S., Jost, R., König, A., Liss, T., Lüßmann, R., May, M., Nonhoff, B., Reichel, B., Strehlow, R., Stamatakis, A., Stuckmann, N., Vilbig, A., Lenke, M., Ludwig, T., Bode, A., and Schleifer, K.-H. (2004) ARB: a software environment for sequence data. *Nucleic Acids Res.* 32:1363–1371.

Luzapone, C. and Knight, R. (2005) UniFrac: a new phylogenetic method for comparing communities. *Appl. Environ. Microbiol.* 71:8228–8235.

Pentecost, A. and Riding, R. (1986) Calcification in cyanobacteria. In *Biomineralization in Lower Plants and Animals,* Systematics Association Special Volume, Vol. 30, edited by B.S.C. Leadbeater and R. Riding, Clarendon Press, Oxford, pp 73–90.

Perry, T.D., Klepac-Ceraj, V., Zhang, X.V., McNamara, C.J., Polz, M.F., Martin, S.T., Berke, N., and Mitchell, R. (2005) Binding of harvested bacterial exopolymers to the surface of calcite. *Environ. Sci. Technol.* 39:8770–8775.

Perry, R.S., McLoughlin, N., Lynne, B.Y., Sephton, M.A., Oliver, J.D., Perry, C.C., Campbell, K., Engel, M.H., Farmer, J.D., Brasier, M.D., and Staley, J.T. (2007) Defining biominerals and organominerals: direct and indirect indicators of life. *Sediment. Geol.* 201:157–179.

Schloss, P.D., Larget, B.R., and Handelsman, J. (2004) Integration of microbial ecology and statistics: a test to compare gene libraries. *Appl. Environ. Microbiol.* 70:5485–5492.

Singleton, D.R., Furlong, M., Rathbun, S.L., and Whitman, W.B. (2001) Quantitative comparisons of 16S rRNA gene sequence

libraries from environmental samples. *Appl. Environ. Microbiol.* 67:4374–4376.

Spear, J.R., Walker, J.J., McCollom, T.M., and Pace, N.R. (2005) Hydrogen and bioenergetics in the Yellowstone geothermal ecosystem. *Proc. Natl. Acad. Sci. U.S.A.* 102:2555–2560.

Stackebrandt, E. and Goebel, B.M. (1994) Taxonomic note: a place for DNA-DNA hybridization and 16S rRNA sequence analysis in the present species definition in bacteriology. *Int. J. Syst. Evol. Microbiol.* 44:846–849.

van Lith, Y., Vasconcelos, C., Warthmann, R., and Martins, J.C.F. (2002) Bacterial sulfate reduction and salinity: two controls on dolomite precipitation in Lagoa Vermelha and Brejo de Espinho (Brazil). *Hydrobiologia* 485:35–49.

Visscher, P.T. and Stolz, J.F. (2005) Microbial mats as bioreactors: populations, processes, and products. *Palaeogeogr., Palaeoclimatol., Palaeoecol.* 219:87–100.

Visscher, P.T., Prins, R.A., and van Gemerden, H. (1992) Rates of sulfate reduction and thiosulfate consumption in a marine microbial mat. *FEMS Microbiol. Ecol.* 86:283–294.

Visscher, P.T., Reid, R.P., Bebout, B.M., Hoeft, S.E., MacIntyre, I.G., and Thompson, J.A. (1998) Formation of lithified micritic laminae in modern marine stromatolites (Bahamas): the role of sulfur cycling. *Am. Mineral.* 83:1482–1492.

Visscher, P.T., Reid, R.P., and Bebout, B.M. (2000) Microscale observations of sulfate reduction: correlation of microbial activity with lithified micritic laminae in modern marine stromatolites. *Geology* 28:919–922.

Wotton, R.S. (2004) The ubiquity and many roles of exopolymers (EPS) in aquatic systems. *Sci. Mar.* 61(Supplement 1):13–21.

Walter, L.M., Bishof, S.A., Patterson, W.P., and Lyons, T.W. (1993) Dissolution and recrystallization in modern shelf carbonates: evidence from pore water and solid phase chemistry. *Philos. Trans. R. Soc. Lond., A* 344:27–36.

Address correspondence to:
Pieter T. Visscher
1080 Shennecossett Rd.
Groton, CT
USA

E-mail: pieter.visscher@uconn.edu